Int. J. Heat Mass Transfer. Vol. 6, pp. 841–852. Pergamon Press 1963. Printed in Great Britain.

SIMULTANEOUS HEAT TRANSFER IN A CIRCULAR TUBE BY FREE-MOLECULE CONVECTION AND THERMAL RADIATION

E. M. SPARROW and V. K. JONSSON
Heat Transfer Laboratory, University of Minnesota, Minneapolis, Minn.

(*Received* 4 *December* 1962 *and in revised form* 6 *March* 1963)

Abstract—A general analysis including arbitrary thermal boundary conditions has been made for the energy transport in a circular tube in which a highly rarefied gas is flowing. Thermal radiation acts simultaneously with the free-molecule convection. Detailed consideration was given to the cases of uniform wall temperature, uniform wall heat flux, and the adiabatic wall. It was found that at all temperature levels except those well below room temperature, the results corresponding to combined convective and radiative transport differ little from those for purely radiative transport. Whenever results for the purely radiative transport differed appreciably from those of the purely convective transport, the radiation appeared to be the dominant mode in the simultaneous transport process.

NOMENCLATURE

A, surface area;
a, accommodation coefficient;
d, tube diameter;
e, convective energy/time-area;
F, angle factor;
g, solution of equation (12);
h, solution of equation (16);
I, integral defined by equation (13);
L, tube length;
m, mass flux/time-area;
p, pressure;
Q, overall heat flux/time;
q, local heat flux/time-area;
q_0, uniform heat flux;
R, gas constant;
T, absolute temperature;
T_0, uniform wall temperature;
X, dimensionless co-ordinate, x/d;
x, axial co-ordinate.

Greek symbols

α, absorptivity;
β, ratio of convective to radiative energy efflux;
γ, specific heat ratio;
ϵ, emissivity;
θ, energy variable, equation (9a);
ξ, ξ', dummy integration variables;
ρ, reflectivity;
σ, Stefan–Boltzmann constant.

Subscripts

1, reservoir 1;
2, reservoir 2;
r, rad, radiative;
m, mol, molecular.

INTRODUCTION

THIS paper is concerned with the simultaneous energy transport by convection and radiation in a rarefied gas. Consideration will be given to the free-molecule regime, wherein the density level is such that the molecular mean free path is much larger than a typical apparatus dimension. The energy transport will be studied here for the case of the circular tube. The mass flow in a circular tube under free-molecule conditions has already been investigated in some detail. This work is summarized in [1], which is also devoted to demonstrating a useful analogy between the transfer of both mass and energy in a rarefied gas and the transfer of energy by thermal radiation. To demonstrate the analogy, the energy throughflow and surface temperature distribution associated with the convective transport were calculated for the case of the adiabatic tube wall. Pure radiative transport through tubes has been studied by a number of investigators [2, 3, 4]. To the knowledge of the authors, the problem of simultaneous transport has heretofore not been analysed.

To get a feeling for the relative magnitudes of

the energy quantities involved, it is instructive to compare the equilibrium energy fluxes streaming from an isothermal cavity (temperature T, pressure p) by radiation and by free-molecule convection. The rate of radiative efflux per unit area is σT^4, while the rate of convective energy transport e per unit area is [5]

$$e = 0{\cdot}5R\left[\frac{(\gamma+1)}{(\gamma-1)}\right]mT \tag{1}$$

in which m, the mass flux per unit area, has the value

$$\frac{p}{\sqrt{(2\pi RT)}} \tag{2}$$

for equilibrium efflux from an isothermal cavity. Then, forming the ratio (to be called β) of the free-molecule to the radiative flux, there follows

$$\beta = \frac{mR(\gamma+1)}{2(\gamma-1)\sigma T^3}. \tag{3}$$

For air at 500°R (room temperature), $\beta = 10^5 p$ (atm). For a tube diameter of 0·1 in, pressures no greater than 2 μ Hg ($2{\cdot}6 \times 10^{-6}$ atm) would probably insure free-molecule conditions; while for a tube diameter of 1 in, pressures of 0·2 μ Hg and less would be required.* The corresponding room-temperature β values would be 0·26 and 0·026. Since $\beta \sim T^{-3{\cdot}5}$, it is seen that β becomes larger at low temperatures and becomes smaller at high temperatures.

A schematic diagram of the circular tube system under consideration here is shown in Fig. 1. A tube of diameter d and length L connects two reservoirs. The reservoirs are large enough to achieve internal thermodynamic equilibrium, and the reservoir pressures are maintained by pumps in an external flow circuit. The emission and reflection of thermal radiation and the reflection of mass at the tube wall is assumed to be diffuse.

GENERAL ANALYSIS

The local rate of heat transfer q at any location along the tube surface is the sum of radiative q_r and free-molecular q_m contributions,

$$q = q_r + q_m \tag{4}$$

* Ratio of mean free path to diameter is 10.

in which the heat fluxes are positive when heat flows out of the surface. It is now necessary to relate q_r and q_m to the thermal and flow parameters of the system. These derivations are quite lengthy, and only a general outline will be given. For the net radiative flux q_r at some location x (area dA_x) there are the following contributions to be considered: (a) the emission,

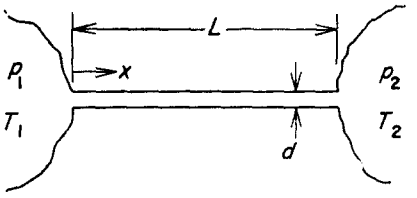

FIG. 1. Schematic of the circular tube system.

$\epsilon\sigma T^4(x)$; (b) the radiation from the reservoirs 1 and 2 which is directly incident and is absorbed at x; (c) the radiation coming from all other surface locations on the tube wall which arrives and is absorbed at x. Because there is thermal equilibrium in the reservoirs, the radiation streaming into the tube is black-body radiation which is uniformly and diffusely distributed across the sections at $x = 0$ and $x = L$. From reservoir 1, an energy flux $\sigma T_1^4 F_{x-1}$ arrives at x per unit time and area; the corresponding quantity from reservoir 2 is $\sigma T_2^4 F_{x-2}$. Of these, a fraction α is absorbed. The absorbed energy flux discussed in item (c) requires a somewhat lengthy derivation which will be omitted here. Putting together the various contributions to q_r and additionally assuming gray-body conditions ($\epsilon = \alpha$), there is obtained

$$q_r(X) = \alpha\sigma T^4(X) - \alpha\sigma T_1^4 F_{X-1} - \alpha\sigma T_2^4 F_{X-2} - \alpha\sigma\int_0^{L/d} T^4(\xi)\,dF_{X-\xi} + (1-\alpha)\int_0^{L/d} q_r(\xi)\,dF_{X-\xi}. \tag{5}$$

The last term on the right represents the energy absorbed at X due to inter-reflected radiation.

The heat flux q_m for the molecular convection is most easily derived by analogy with the radiation balance of equation (5). In fact, it is only necessary to replace α by the accommodation coefficient a and σT^4 by the convective energy

flux e. This latter quantity is related to the temperatures and pressures of the system in accordance with equation (1), in which mass flux m has the following forms depending on whether e_1, e_2, or $e(x)$ is being described

$$m_{1,2} = \frac{p_{1,2}}{\sqrt{(2\pi R T_{1,2})}},$$
$$m(x) = m_1 f(x) + m_2 f(L - x). \quad (6)$$

The f function has been calculated in [1].

If the surface temperature is prescribed, then equation (5) becomes an integral equation for determining q_r without recourse to the q_m. Similarly, the q_m equation is independent of the radiation process. The separate solutions for q_r and q_m can be added together in accordance with equation (4), and the local heat flux q corresponding to the prescribed surface temperature thus obtained.

For prescribed heat flux q, the foregoing equations are not at all convenient since the separate components q_r and q_m would, in general, not be known. It is therefore necessary to proceed further. After a rather lengthy development, it was found possible to combine the q_r and q_m equations with the aid of (4). The result is a single, albeit highly complex, integral equation involving T and q.

$$\begin{aligned} -q(X) + \alpha\sigma T^4(X) + ae(X) - \Lambda(X) \\ = \sigma \int_0^{L/d} T^4(\xi)[\alpha(2 - a)\, \mathrm{d}F_{X-\xi} \\ - \alpha(1 - a)\, \mathrm{d}K(\xi, X)] \\ + \int_0^{L/d} e(\xi)[a(2 - \alpha)\, \mathrm{d}F_{X-\xi} \\ - a(1 - \alpha)\, \mathrm{d}K(\xi, X)] \\ - \int_0^{L/d} q(\xi)\{[(1 - a) + (1 - \alpha)]\, \mathrm{d}F_{X-\xi} \\ - (1 - a)(1 - \alpha)\, \mathrm{d}K(\xi, X)\} \end{aligned} \quad (7)$$

in which $\Lambda(X)$ represents a known function of X,

$$\begin{aligned} \Lambda(X) = (\alpha\sigma T_2^4 + ae_2)F_{X-2} - [\alpha(1 - a)\sigma T_2^4 \\ + a(1 - \alpha)e_2] \int_0^{L/d} F_{\xi-2}\, \mathrm{d}F_{X-\xi} \\ + (\alpha\sigma T_1^4 + ae_1)F_{X-1} - [\alpha(1 - a)\sigma T_1^4 \\ + a(1 - \alpha)e_1] \int_0^{L/d} F_{\xi-1}\, \mathrm{d}F_{X-\xi} \end{aligned} \quad (7a)$$

and $\mathrm{d}K$ is an abbreviation for

$$\mathrm{d}K(\xi, X) = \int_{\xi'=0}^{L/d} \mathrm{d}F_{\xi'-\xi}\, \mathrm{d}F_{X-\xi'}, \quad (7b)$$

with ξ' a dummy integration variable.

If q is prescribed, then in principle, the temperature distribution $T(X)$ can be solved for from equation (7). However, the practical aspects of obtaining solutions are quite formidable. First of all, the equation is nonlinear. Numerical treatment would almost certainly be required, especially since the $f(X)$ functions appearing in the $e(X)$ are available numerically. Even for the simplest problem of uniform wall heat flux $q(X) = q_0$ there would be seven independent parameters which would have to be specified for each numerical solution.

$$\frac{q_0}{\sigma T_1^4},\ \frac{T_2}{T_1},\ \frac{p_2}{p_1},\ \beta_1 = \frac{m_1 R(\gamma + 1)}{2(\gamma - 1)\sigma T_1^3},\ \frac{L}{d},\ \alpha,\ a. \quad (8)$$

If only two values of each parameter were considered, this would amount to 128 (2^7) separate cases. The computational effort for the general situation $\alpha \neq a$ is clearly enormous.

For the special situation in which $\alpha = a$, a significant simplification results. Upon adding the q_r and q_m equations and noting that $q = q_r + q_m$,

$$\begin{aligned} \frac{q(X)}{a} = \theta(X) - \theta_1 F_{X-1} - \theta_2 F_{X-2} \\ - \int_0^{L/d} \theta(\xi)\, \mathrm{d}F_{X-\xi} + (1 - a) \int_0^{L/d} \frac{q(\xi)}{a}\, \mathrm{d}F_{X-\xi} \end{aligned} \quad (9)$$

in which

$$\theta = e + \sigma T^4. \quad (9a)$$

For a prescribed heat flux $q(X)$, equation (9) is a *linear* integral equation for $\theta(X)$. The linearity means that separate solutions can be obtained corresponding to each of the inhomogeneous terms [i.e. terms not containing $\theta(X)$], and the separate solutions are added to give the complete solution. In this way, the number of parameters which must be prescribed for a given numerical solution are substantially reduced. Also, the linearity of the equation contributes to the certainty that a numerical solution can be obtained.

DISCUSSION

In deciding on a reasonable direction for the numerical work, it is appropriate to look at the properties of typical engineering materials. Surfaces which may be expected to emit and reflect infra-red radiation in an approximately

diffuse manner include non-metals, metallic oxides, and perhaps very rough metallic surfaces. Such surfaces have moderate or high values for the absorptivity coefficient α. On the other hand, experimental values of the accommodation coefficient a for various gases on engineering surfaces which have not been physically and chemically cleaned and purged of adsorbed gases tend to be high. In the light of the foregoing discussion, it would appear that the values of α and a appropriate to an analysis based on diffusely distributed radiation should not be greatly different.

For the case of prescribed surface temperature, the heat fluxes due to radiant transport and to free-molecule transport can be determined separately. The combined heat flux can then be found by summing these separate contributions for any α or a, but as described above, the results have practical meaning only for moderate and high values of α and a.

For the case of prescribed heat flux, it would be necessary to deal with equation (7) for the case of $\alpha \neq a$. When $\alpha = a$, then equation (9) can be applied. In view of the foregoing consideration of the magnitudes of α and a, and taking the complexity of (7) into account, the authors are persuaded that (9) is a more appropriate starting point for numerical consideration than is (7). From the results to be presented in later sections, it will be seen that for surfaces which can realistically be considered as diffuse, there is little motivation to pursue the refinements (i.e. $\alpha \neq a$) contained in equation (7).

In the following section, consideration will be given to the uniform wall temperature problem. Subsequent sections will treat the uniform heat flux problem and the adiabatic wall problem.

UNIFORM WALL TEMPERATURE

For the case of uniform wall temperature, $T(X) = T_0$, the governing equation (5) for the radiative heat transfer can be simplified by using the identity $\int_0^{L/d} \mathrm{d}F_{X-\xi} = 1 - F_{X-1} - F_{X-2}$, and the solution may be written

$$\frac{q_r(X)}{a} = \sigma(T_0^4 - T_1^4)g_\alpha(X) + \sigma(T_0^4 - T_2^4)g_\alpha\left(\frac{L}{d} - X\right). \quad (10)$$

Similarly, the result for q_m is

$$\frac{q_m(X)}{a} = \left(\frac{T_0}{T_1} - 1\right)e_1 g_a(X) + \left(\frac{T_0}{T_2} - 1\right)e_2 g_a\left(\frac{L}{d} - X\right). \quad (11)$$

The g function appearing in the foregoing is obtained by solving

$$g_i(X) = F_{X-1} + (1 - i)\int_0^{L/d} g_i(\xi)\,\mathrm{d}F_{X-\xi}. \quad (12)$$

To complete the heat-transfer results, it still remains to supply the g functions. These have been found by solving equation (12)* for L/d values ranging from 1/4 to 32 and for a or α values ranging from 0·2 to 1. This information is presented graphically on Figs. 2 and 3, the first of which pertains to smaller L/d while the last pertains to larger L/d.

For short tubes, the g function varies only slightly with x. Correspondingly, the heat flux should have only a moderate x dependence. For long tubes, the g function is essentially zero throughout the entire tube, except for the region near the end where there is a rapid variation. The heat transfer should also vary rapidly near the end and be essentially zero elsewhere. The level of the g curves is lower with increasing α or a. However, the effect of this on $q(x)$ is opposed by the factors of α and a which appear in equations (10) and (11).

With the information provided in Figs. 2 and 3, the local heat flux q can now be calculated by adding the q_r and q_m. Inspection of the final equation for q reveals the presence of seven independent dimensionless parameters as well as x/d. In any reasonable amount of space, it is not possible to provide plots which will demonstrate the complete parametric dependence of the heat transfer. The best that one can do is to try to establish some feeling for the trends. Such a discussion can be carried out in a somewhat simpler way for the soon-to-be-presented overall heat-transfer results in which x/d dependence does not appear.

The rate Q at which heat is transferred from the entire tube wall may be found by integrating

* The required angle factors may be found in [1], equations (7a), (7b) and (11).

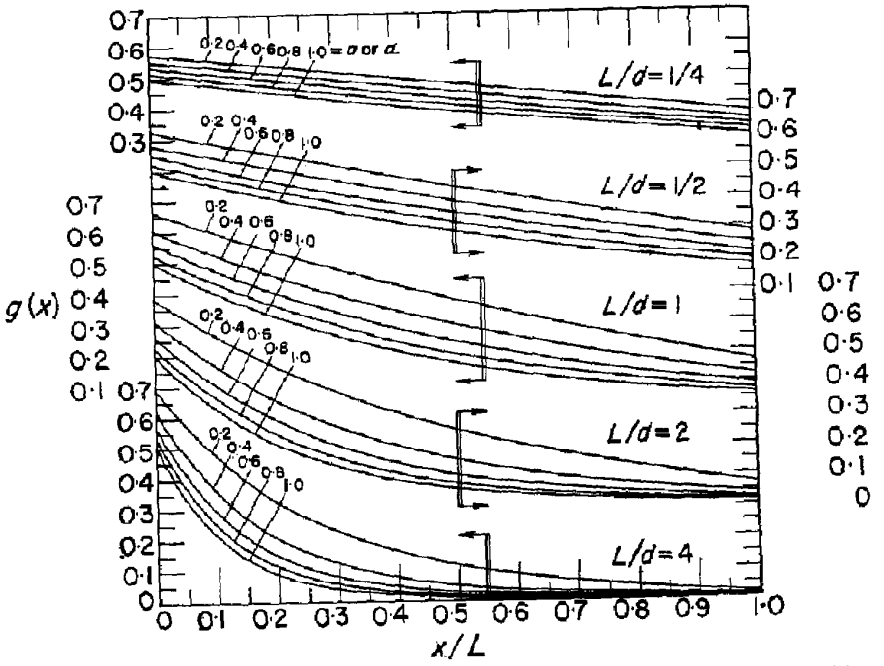

FIG. 2. The g function for the uniform wall temperature problem, range of small L/d.

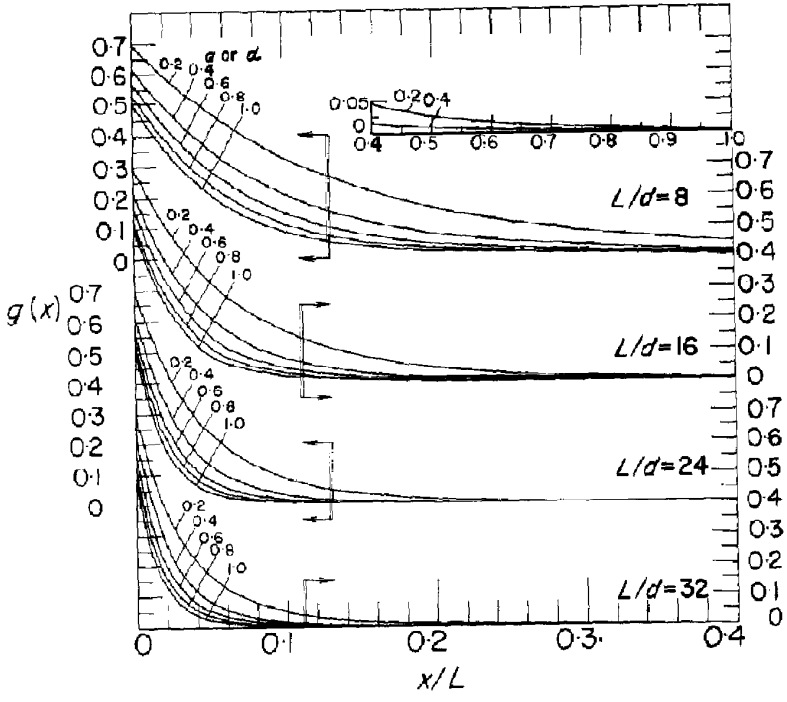

FIG. 3. The g function for the uniform wall temperature problem, range of large L/d.

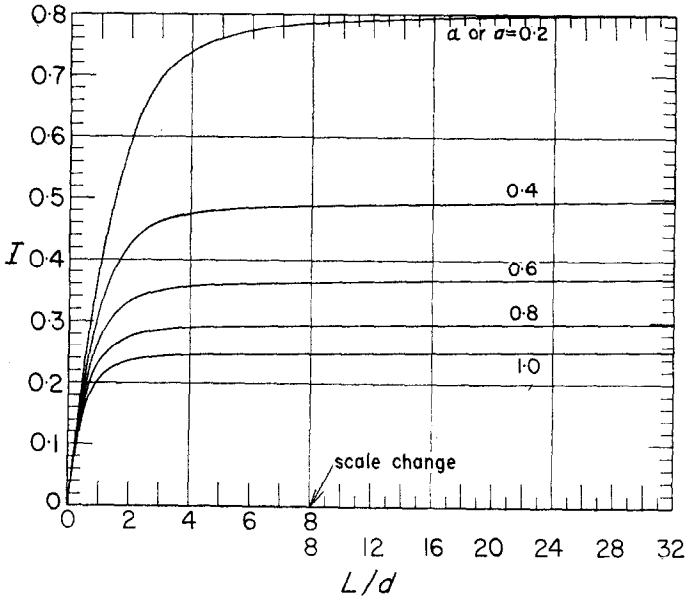

FIG. 4. The I integral for the overall heat-transfer calculation.

the local heat flux q, $Q = \int_0^L q(x)\pi d\,(\mathrm{d}x)$. Carrying out the integration and introducing the abbreviation

$$I_i = \int_0^{L/d} g_i(X)\,\mathrm{d}X = \int_0^{L/d} g_i\left(\frac{L}{d} - X\right)\mathrm{d}X \quad (13)$$

there results

$$\frac{Q}{\sigma T_1^4 \pi d^2} = \alpha I_\alpha \left[2\left(\frac{T_0}{T_1}\right)^4 - \left(\frac{T_2}{T_1}\right)^4 - 1\right]$$
$$+ a\beta_1 I_a \left[\frac{T_0}{T_1} - 1 + \left(\frac{T_0}{T_2} - 1\right)\frac{p_2}{p_1}\sqrt{\left(\frac{T_2}{T_1}\right)}\right] \quad (14)$$

in which the subscripts α and a identify the parameter on which I depends. The numerical values of I have been plotted on Fig. 4 as a function of the tube length–diameter ratio for parametric values of α or a. The most striking feature of this graph is the fact that I is relatively independent of L/d except for short tubes. Considering equation (14), this implies that for tubes which are not too short, the overall heat transfer is relatively insensitive to changes in the length. For instance, the heat transfer from a tube having $L = 15d$ is less than 1 per cent different from a tube having $L = 30d$.

To get some feeling for the effect of the dimensionless parameters, Figs. 5 and 6 have been prepared. The figures show the overall heat transfer as a function of β_1 in the range between 0 and 2. Fig. 5 is devoted to a typical short tube, $L/d = 1$; while Fig. 6 is typical of a long tube, $L/d = 24$. Curves are shown for two temperature conditions: $T_0/T_1 = T_2/T_1 = 1{\cdot}1$ (solid lines) and $T_0/T_1 = T_2/T_1 = 1{\cdot}6$ (dashed lines), and a variety of α and a values. The $\beta_1 = 0$ case corresponds to purely radiative transport, and the curves have been normalized by the heat transfer Q_{rad} for pure radiation. Therefore, the deviations of Q/Q_{rad} from unity give a direct measure of the effects of free-molecule convection.

From the figures it is seen that for small values of β_1, the free-molecule transport contributes to a rather small increase in the heat transfer relative to that for pure radiation. Recalling (from the Introduction) that for room temperature and typical pressures, $\beta_1 \sim 0{\cdot}025$–$0{\cdot}25$, and noting further that $\beta_1 \sim T^{-3{\cdot}5}$, it follows that the radiative transport clearly dominates at temperatures above room temperature. At lower temperatures and higher

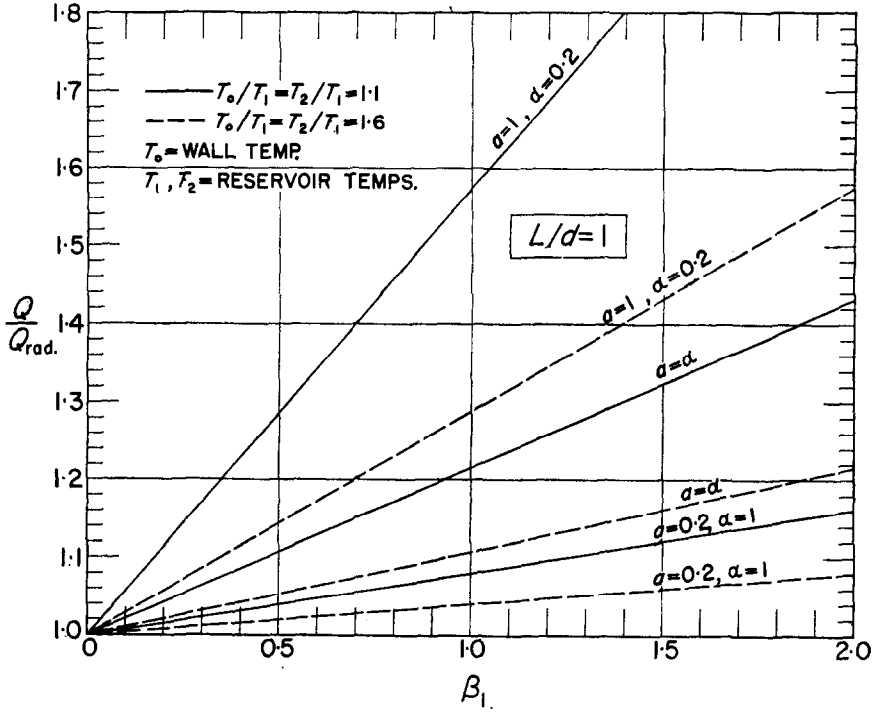

FIG. 5. Illustrative overall heat-transfer results for the uniform wall temperature case, $L/d = 1$.

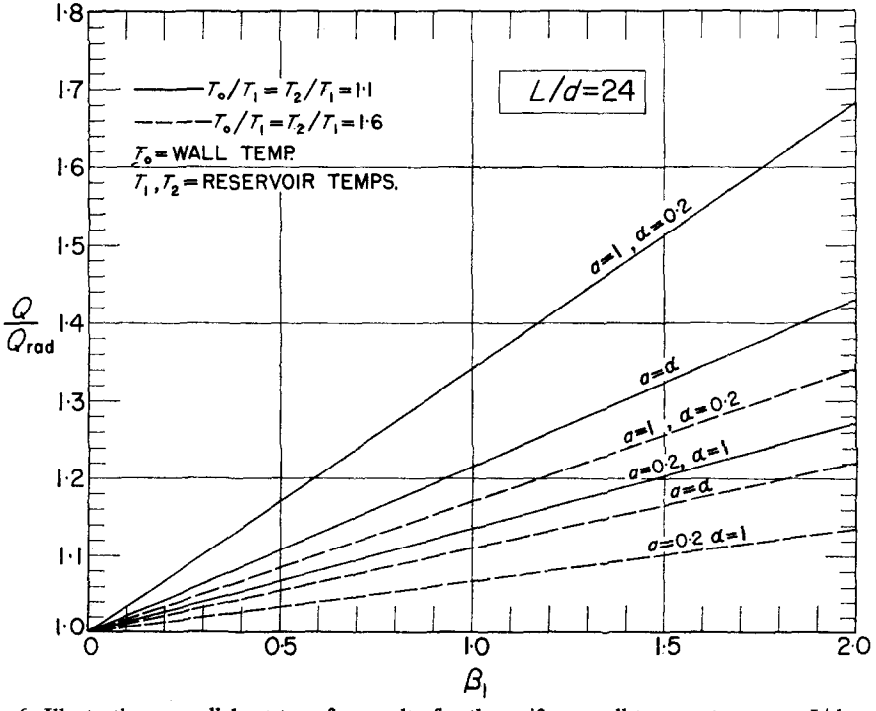

FIG. 6. Illustrative overall heat-transfer results for the uniform wall temperature case, $L/d = 24$.

pressure levels* β_1 can grow larger, but radiation should still be dominant for α and a values at which the assumption of diffuse reflection is reasonable.

The trends for the short tube (Fig. 5) are also in evidence for the long tube (Fig. 6). But, there is one marked difference. Namely, that for the long tube, the results are much less influenced by the detailed values of a and α. It may additionally be noted from Fig. 4 that tubes of moderate length already behave like long tubes.

UNIFORM WALL HEAT FLUX

As previously discussed, consideration of the uniform heat flux case will be specialized to the situation $\alpha = a$. To determine the wall temperature corresponding to the prescribed heat flux q_0, the first step is to solve equation (9) for the θ distribution and then, with this $\theta(X)$ as input, the next step is to solve the quadratic equation (9a) for $T(X)$.

The solution of equation (9) is facilitated by its linearity.

$$\theta(X) = e(X) + \sigma T^4(X) = \theta_1 f(X) + \theta_2 f\left(\frac{L}{d} - X\right) + q_0\left[\frac{1-a}{a} + h(X)\right] \quad (15)$$

* Smaller apparatus dimensions would be required to achieve free-molecule conditions at higher pressures.

in which

$$h(X) = 1 + \int_0^{L/d} h(\xi)\, dF_{x-\xi}. \quad (16)$$

Additionally, in deriving equation (15), the identity $f(X) + f(L/d - X) = 1$ has been used [1]. Then, by introducing the definitions of θ and e and rearranging, one can derive

$$\left[\frac{T(X)}{T_1}\right]^4 + \beta_1\left[f(X) + \frac{p_2}{p_1}\sqrt{\left(\frac{T_1}{T_2}\right)} f\left(\frac{L}{d} - X\right)\right]\frac{T(X)}{T_1} = (1+\beta_1) f(X) + f\left(\frac{L}{d} - X\right)\left[\frac{p_2}{p_1}\sqrt{\left(\frac{T_2}{T_1}\right)}\beta_1 + \left(\frac{T_2}{T_1}\right)^4\right] + \frac{q_0}{\sigma T_1^4}\left[\frac{1-a}{a} + h(X)\right]. \quad (17)$$

This is a fourth degree algebraic equation, the solution to which gives the distribution of the wall temperature as a function of position along the tube. The f function needed in this calculation is plotted on Fig. 2 of [1] for L/d values up to 24. For larger L/d, it is sufficient to use $f(X) = 1 - (d/L)X$. The h function has been determined as part of this investigation and is plotted on Fig. 7 as a function of x/L. The curves

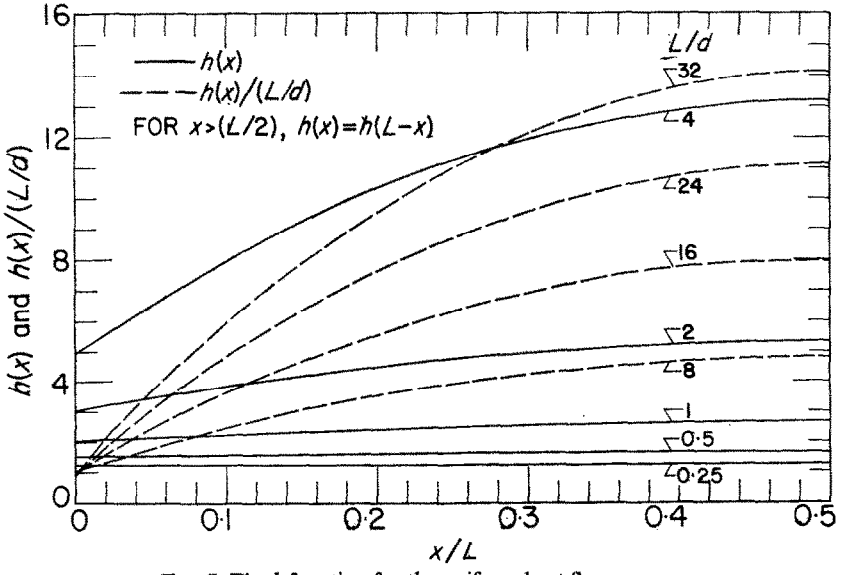

FIG. 7. The h function for the uniform heat flux case.

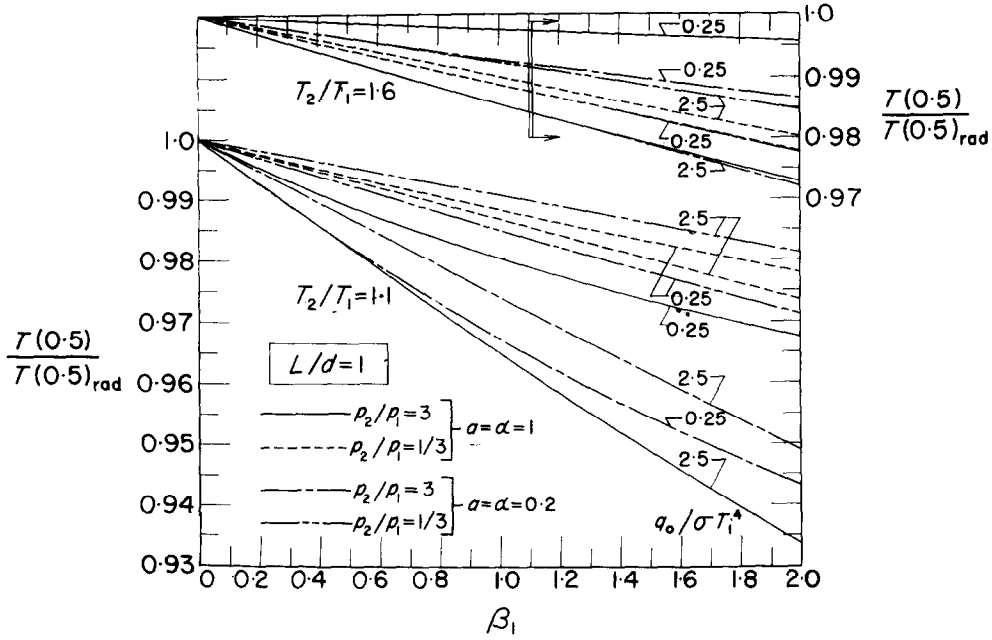

FIG. 8. Illustrative wall temperature results for the uniform heat flux case, $L/d = 1$.

correspond to L/d values ranging from 1/4 to 32. The figure shows that in addition to an increase in level with L/d, the h function also varies strongly with position for the longer tubes—the larger values being at the center of the tube ($x = 0{\cdot}5L$). That this is physically plausible may be understood by noting that h is directly related to the distribution of the tube wall temperature corresponding to the case of uniform wall heat flux [4].

The surface temperature distribution depends upon prescribed values of six independent parameters, equation (17). Once again, space limitations preclude a presentation of the complete parametric dependence of the results. However, to provide an insight into trends, the illustrative Figs. 8 and 9 have been prepared. Attention is directed first to Fig. 8, which is meant to typify short tubes. Here, there is plotted the wall temperature at the mid-plane ($x = 0{\cdot}5L$) as a function of energy flux ratio β_1 for parametric values of T_2/T_1, p_2/p_1 and $\alpha(=a)$. The mid-plane temperature has been normalized by the temperature T_{rad} which would exist at this location if radiative transport acted alone. Therefore, the deviation of the curves from unity immediately gives the effect of free-molecule convection. Working plots (not shown here) for locations $x = 0$ and $x = L$ in the $L/d = 1$ tube are qualitatively similar to Fig. 8 and differ quantitatively only to a small extent. This is to be expected in a short tube.

The first point to be noted in appraising Fig. 8 is the rather expanded ordinate scale. Corresponding to the prior estimate of 0·025–0·25 for β_1 at room temperature, it is seen from the figure that the wall temperature is very little different from that which would exist for purely radiative transport. Even for higher β_1 values (lower temperature levels), the deviations from T_{rad} are not appreciable in most cases. There are a few curves, all for $p_2/p_1 = 3$, which indicate moderate deviations from T_{rad} at the larger β_1 values. However, since $\beta_1 \sim p_1$, it is not likely that large β_1 and large p_2/p_1 will occur simultaneously. The results of Fig. 8 were calculated for the condition $\alpha = a$. It is expected that the deviations of T from T_{rad} will not be large at small β_1 for any α and a consistent with the diffuse model.

Fig. 9, typical of long tubes, is constructed somewhat differently from Fig. 8. This is

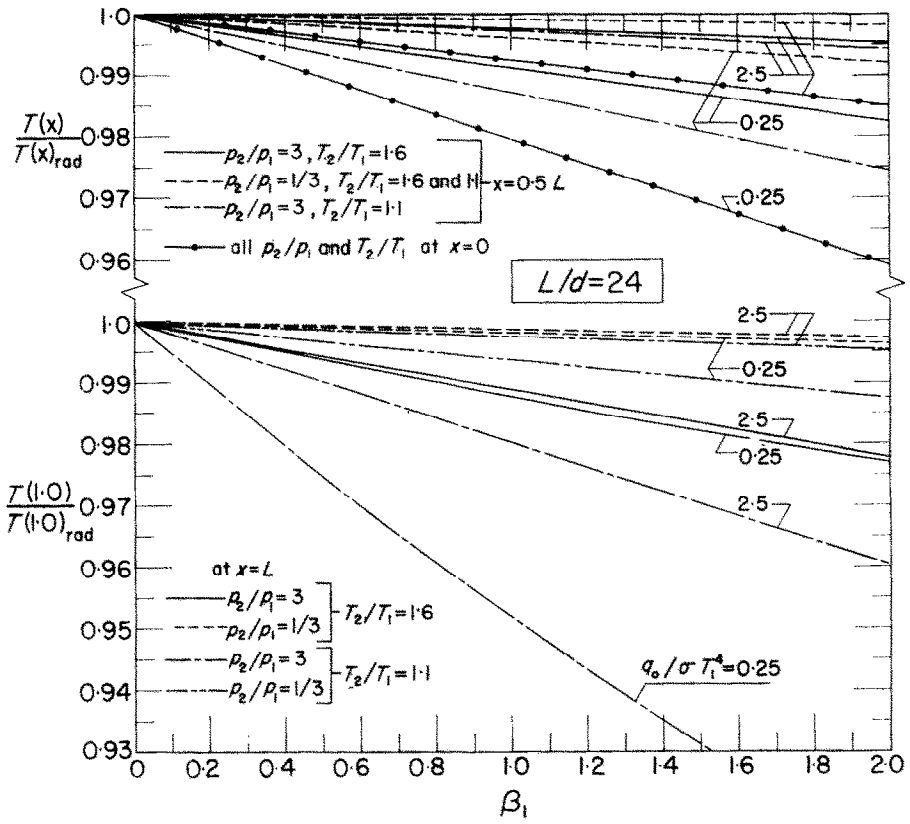

FIG. 9. Illustrative wall temperature results for the uniform heat flux case, $L/d = 24$.

necessary because the T/T_{rad} ratio is now a stronger function of position. The lower part of the figure is devoted to $x = L$, while the upper part is for $x = 0$ and $x = 0{\cdot}5L$. Expanded ordinate scales are employed as before. An important feature of Fig. 8 is the fact that the dependence of the T/T_{rad} ratio on α is essentially negligible. In fact, the term $(1 - a)/a$ may be deleted from equation (17) without loss, for values of α and a that are realistic for the condition of diffuse reflection and emission. In effect, this removes the restriction that $\alpha = a$. The deviations of T/T_{rad} from unity are seen to be small for room temperature β_1 values (0·025–0·25). The lowest curve on the figure indicates that cases do exist where large deviations are possible provided that β_1 and p_2/p_1 are both large; but as previously discussed, this is not a too likely situation.

ADIABATIC WALL

The adiabatic wall condition can be treated as a special case of the uniform heat flux analysis merely by setting $q_0 = 0$ in equation (17). These results depend on four parameters: T_2/T_1, p_2/p_1, L/d, and β_1. As before, there are too many parameters for a detailed graphical presentation, and representative cases will be selected to show trends.

Fig. 10 presents adiabatic wall temperature results for $L/d = 1$, a typical short tube. The upper part of the figure is for $T_2/T_1 = 1{\cdot}1$, while the lower part is for $T_2/T_1 = 1{\cdot}6$. Curves are given for three locations: $x = 0$, $x = 0{\cdot}5L$, and $x = L$. The results are normalized by the adiabatic wall temperature for pure radiation, T_{rad}. The deviations of T from T_{rad} are seen to be small indeed. It might at first appear that this is because the radiation dominates over the

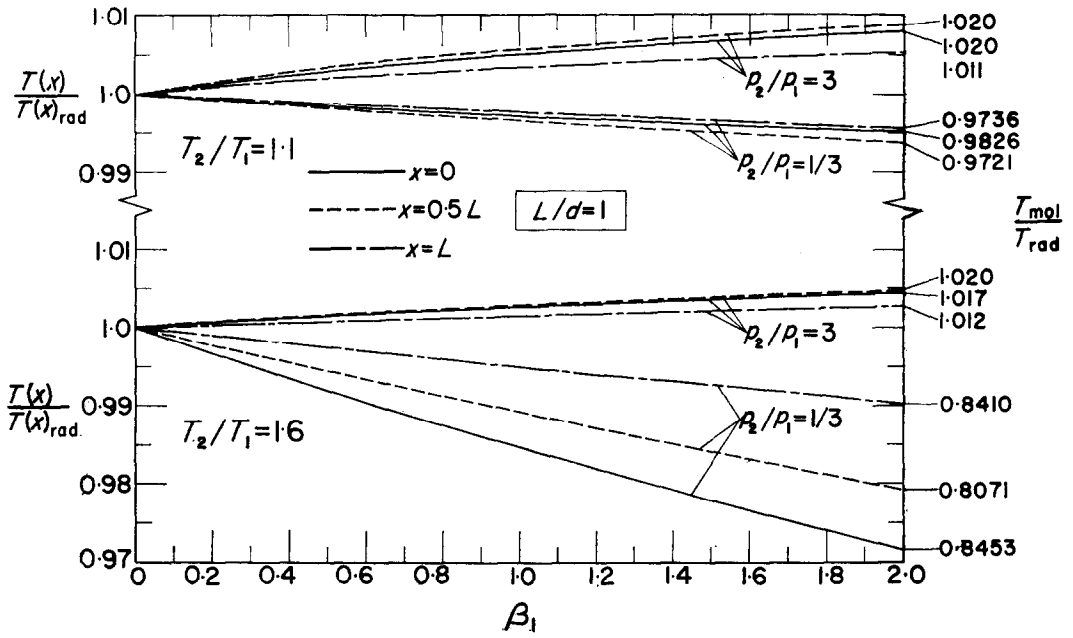

FIG. 10. Illustrative adiabatic wall temperature results, $L/d = 1$.

molecular transport. However, this is not necessarily so. To check this matter, the ratios of T_{mol} (the adiabatic wall temperature for pure molecular transport) to T_{rad} have been calculated and are listed in the right-hand margin of Fig. 10. It is seen that for most cases, T_{mol} and T_{rad} are not very different. It is therefore reasonable that the adiabatic wall temperature which results when both processes are operating simultaneously will not be very different from either T_{mol} or T_{rad}. For those few cases where T_{mol} and T_{rad} are significantly different, the radiative transport appears to be dominant. This conclusion ought also to hold for $a \neq \alpha$ which are realistic for diffuse surfaces.

The findings for the long tube can be stated without the assistance of an additional figure. At locations near the ends, T_{mol} and T_{rad} are almost equal, and therefore, the temperature which exists when both processes operate simultaneously will differ very little from either. At the central plane, $x = 0{\cdot}5L$, the dashed curves of Fig. 10 also apply to the long tube. As before, whenever T_{mol} and T_{rad} are appreciably different, the radiative transport wins out.

REFERENCES

1. E. M. SPARROW, V. K. JONSSON and T. S. LUNDGREN, Free-molecule tube flow and adiabatic wall temperatures, *J. Heat Transfer*, **C85**, 111–118 (1963).
2. H. BUCKLEY, On the radiation from the inside of a circular cylinder, Part I, *Phil. Mag.* **4**, 23, 753–762 (1927).
3. H. C. HOTTEL and J. D. KELLER, Effect of reradiation on heat transmission in furnaces and through openings, *Trans. ASME*, **55**, 39–49 (1933).
4. C. M. USISKIN and R. SIEGEL, Thermal radiation from a cylindrical enclosure with specified wall heat flux, *J. Heat Transfer, Trans. ASME*, C **82**, 369–374 (1960).
5. S. A. SCHAAF and P. L. CHAMBRÉ, Flow of rarefied gases. High Speed Aerodynamics and Jet Propulsion, Princeton University Press, Section H, Vol. 3, (1958).
6. J. P. HARTNETT, *A Survey of Thermal Accommodation Coefficients*, Advances in Applied Mechanics, Supplement 1, Rarefied Gas Dynamics, pp. 1–28. Academic Press, New York (1961).
7. H. Y. WACHMAN, The thermal accommodation co, efficient, a critical survey, *J. Amer. Rocket Soc.* **32**-2–12 (1962).

Résumé—Le transport d'énergie dans le cas d'un écoulement très raréfié dans un tube circulaire, avec conditions thermiques aux limites arbitraires, a été étudié d'une manière très générale. Le rayonnement thermique et la convection libre en régime moléculaire libre agissent simultanément. Les cas où la

température de paroi est constante, le flux de chaleur à la paroi est constant et la paroi adiabatique sont étudiés en détail. On trouve que pour tous les niveaux de température, sauf ceux qui sont très en-dessous de la température ambiante, les résultats correspondants au transport mixte par rayonnement et convection diffèrent peu de ceux relatifs au transport par rayonnement pur. Lorsque les résultats du transport par rayonnement pur diffèrent de façon appréciable de ceux relatifs au transport par convection pure, le rayonnement semble être le mode prédominant dans le processus du transport mixte.

Zusammenfassung—Eine allgemeine Analyse, die auch beliebige thermische Randbedingungen einschliesst, wurde für den Energietransport in einem Rohr mit Kreisquerschnitt, in dem hoch verdünntes Gas strömt, durchgeführt. Gleichzeitig mit der Konvektion freier Moleküle wirkt Temperaturstrahlung. Einer eingehenden Betrachtung wurden die Fälle konstanter Wandtemperatur, konstanter Wärmestromdichte durch die Wand und adiabater Wand unterzogen. Bei allen Temperaturen ausser jenen weit unter Raumtemperatur unterschieden sich die Ergebnisse für gleichzeitigen konvektiven und radiativen Energietransport wenig von den Resultaten für rein radiativen Transport. Soweit die Ergebnisse für reinen Strahlungstransport merklich von denen für reinen Konvektionstransport abwichen, schien die Strahlung beim Simultantransport die führende Rolle einzunehmen.

Аннотация—Проведен общий анализ переноса энергии при течении сильно разреженного газа в круглой трубе, включая случай произвольного выбора термических граничных условий. Тепловое излучение происходит одновременно со свободно-молекулярной конвекцией. Подробно рассматриваются случаи равномерной температуры стенки, равномерного теплового потока на стенке и адиабатических условий на стенке. Установлено, что для всех температур, за исключением температур намного ниже комнатной, данные для сложного конвективного и лучистого переноса очень мало отличаются от данных для простого лучистого переноса. В том случае, когда данные для чистого переноса энергии излучением заметно отличаются от данных чистого конвективного переноса, лучистый перенос в общем процессе оказывается преобладающим.